Curvature-Driven Reversible In Situ Switching Between Pinned and Roll-Down Superhydrophobic States for Water Droplet Transportation

Dong Wu, Si-Zhu Wu, Qi-Dai Chen, Yong-Lai Zhang, Jia Yao, Xi Yao, Li-Gang Niu, Jiang-Nan Wang, Lei Jiang, and Hong-Bo Sun**

Artificial superhydrophobic surfaces[1–10] with water contact angles (CAs) greater than 150° have been intensively investigated due to their unique "anti-water" property that could be utilized in a wide range of applications.[11–13] Recent development of intelligent devices, such as microfluidic switches and biomedicine transporters, makes strong demands on surface wettability control, therefore, responsive surfaces have become a significant issue for superhydrophobic studies. Up to now, various smart surfaces have been successfully developed as reversible switches for wettability control through a micro-nanostructured surface on a responsive material.[14–25] These unique tunings of surface wettability greatly contributed to refined control of surface wettability. With the thorough understanding of superhydrophobic phenomenon, superhydrophobic surfaces have been classified into five states[26] according to the details of CA hysteresis, which have been well verified on different samples based on experimental results.[1,8,27–29] Superhydrophobic surfaces in different states show distinctive advantages in varied applications. Hence, efforts have also been devoted to precise tuning between different superhydrophobic states. For example, Lai et al.[23a] investigated superhydrophobic surfaces with controlled adhesion to water droplets by using different kinds of rough surfaces. Li et al.[23b] observed reversible switching between a transitional state (sliding angle of 75°) and the Wenzel superhydrophobic state (high adhesion force) by changing the temperature. This inspired no-loss microdroplet transfer and trace-liquid reactor applications,[15] which usually need precise control of water droplet movement on the same surface from "roll-down" to "pinned" superhydrophobic states. Nevertheless, this no-loss transfer of a given water droplet requires a sensitive in situ tuning of surface wettability. Jiang et al. have reported an in situ control of magnetic droplet movement using extra magnetic field, where the tuning was based not on pure water droplets, but on magnetic liquids.[27]

From the practical point of view, it is still worth pointing out that the above-mentioned tuning approaches usually depend on harsh tuning conditions, such as UV irradiation,[18] electrical current,[19,21] a wide range of temperature,[23] or treatments by chemical solvents.[22,25] They may be not suitable for mild condition applications. For example, enzymes or biological cells in microfluidic devices would be seriously affected under UV irradiation, temperature change, or addition of chemical substances. In addition, most of these tunable surfaces are based on artificially introduced material compositions or particular material species,[18–25] such as azobenzene and metal oxides, which suffer from poor biocompatibility. Therefore, it is urgently desirable to find a simple, environmentally friendly, biocompatible, and safe method for in situ control of the wettability of general superhydrophobic surfaces.

We present here for the first time a novel curvature-driven in situ switching for reversible tuning of surface superhydrophobicity from the pinned to the roll-down state. Experimentally, we found that a superhydrophobic poly(dimethylsiloxane) (PDMS) pillar-array film (CA = 150°) shows very high adhesion force to water droplets, which was named the pinned superhydrophobicity state. When the surface curvature was increased to a certain range, along with a slightly increased CA (up to 160°), the adhesion force and the SA (sliding angle) decreased significantly (SA < 5°), which is a typical feature of the Cassie superhydrophobicity state. Based on this unique switching, an in situ "mechanical hand" for water droplet transportation was proposed. It is well known that most polymeric films are flexible and the curvature can be easily adjusted by simple mechanical pressing. Thus our curvature-driven switching would be a general, simple, harmless, and compatible method for wettability control.

In this work, PDMS, which is widely used in microfluidic devices,[30,31] was chosen as a representative polymeric material for superhydrophobic surface fabrication due to its advantages of flexibility, biocompatibility, nontoxicity, and superior stabilities. Large-area regular PDMS pillar arrays were successfully fabricated through the combination of interference lithography[32,33] and soft lithography (Figures S1 and S2 in the

D. Wu, S.-Z. Wu, Dr. Q.-D.Chen, Dr. Y.-L. Zhang, J. Yao, L.-G. Niu, J.-N. Wang, Prof. H.-B. Sun
State Key Laboratory on Integrated Optoelectronics
College of Electronic Science and Engineering
Jilin University
2699 Qianjin Street, Changchun, 130012, P. R. China
E-mail: hbsun@jlu.edu.cn

X. Yao Prof. L. Jiang
Center of Molecular Sciences
Institute of Chemistry
Chinese Academy of Sciences
Beijing, 10190, P. R. China
E-mail: jianglei@iccas.ac.cn

Prof. H.-B. Sun
College of Physics
Jilin University
119 Jiefang Road, Changchun, 130023, P. R. China

DOI: 10.1002/adma.201001688

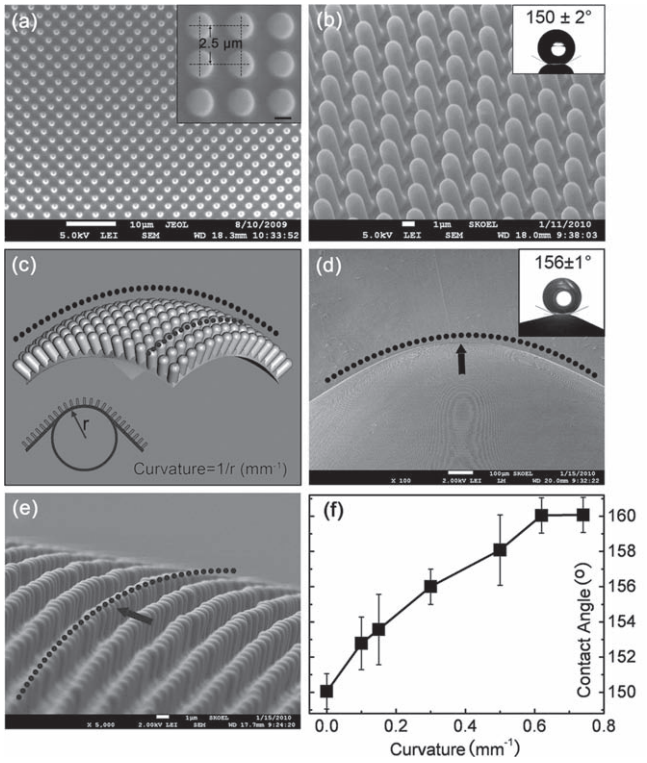

Figure 1. a,b) Top-view and 45°-tilted-view SEM images of a PDMS pillar array (the inset shows the CA of a water droplet). c) Schematic model of the spherical surface of a pillar array and the curvature calculation. d) 90°-tilited-view SEM image of a curved PDMS pillar array (curvature ca. 0.3 mm^{-1}; the inset shows the CA of this curved surface). e) Magnified SEM image of a curved PDMS pillar array. f) The relationship between the curvature and CA.

Supporting Information).[34] **Figure 1a** shows a bird's-eye-view scanning electron microscopy (SEM) image of a regular pillar array with 2.5 μm period (inset of Figure 1a), which has a CA of about 150°, indicating its superhydrophobicity. According to the theoretical wetting model, a pillar array with sharp tips should effectively reduce the contact area between the microstructures and the water droplet and exhibit higher superhydrophobicity. Here, the pillars were designed with round tips, and the array showed higher CA than one with pillars with flat tips (145°), as shown in Figure S6. A tilted-view SEM image of this PDMS pillar array shows that the height of the pillars is about 2.5 μm (Figure 1b). Due to its excellent flexibility, the PDMS film with a uniform pillar array can be deformed reversibly without residual distortion (Figure S3). Figure 1c shows a schematic model of a spherical (curved) surface with a pillar array. Generally, the curved PDMS surface may be considered as a spherical surface, and thus the curvature can be calculated accordingly. As shown in Figure 1d, the radius of curvature is about 3.38 mm and the curvature is calculated to be 0.3 mm^{-1}. Interestingly, the measured CA on this curved surface increases to 156° from initially 150° (flat). The increase of CA is caused by the decrease of the area fraction of the projected wet area f and the simultaneous increment of the roughness factor k. The curvature lengthens the distance between adjacent pillar tips, which leads to the decrease of f. In addition, these pillars are not in a plane after bending, which gives rise to an increase of k. A higher magnification SEM image (Figure 1e) shows that the squarely arranged pillars form an arc-like array on a curved surface. To systemically investigate the relationship between the curvature and the surface wettability, curvatures from 0 mm^{-1} to 0.74 mm^{-1} were designed. As shown in Figure 1f, the CAs gradually increased from 150 ± 2° to 160 ± 2° when the curvature increased to 0.62 mm^{-1}, further demonstrating that the curvature influences the surface wettability. There was no obvious change when the curvature was further increased due to the lack of hierarchical nanostructures on our micrometer-sized pillar arrays.[3,4]

Furthermore, the adhesion between water droplets and curved PDMS pillar arrays was investigated, and further compared with that of a flat pillar array. When a water droplet (4 μL) was in contact with the flat and curved pillar arrays, different adhesion forces were observed, although their CAs were both in the surperhydrophobic range. Shown in **Figure 2b** is the force–distance curves before and after a water microdroplet (4 mL) contacted the flat and curved surfaces. The adhesive

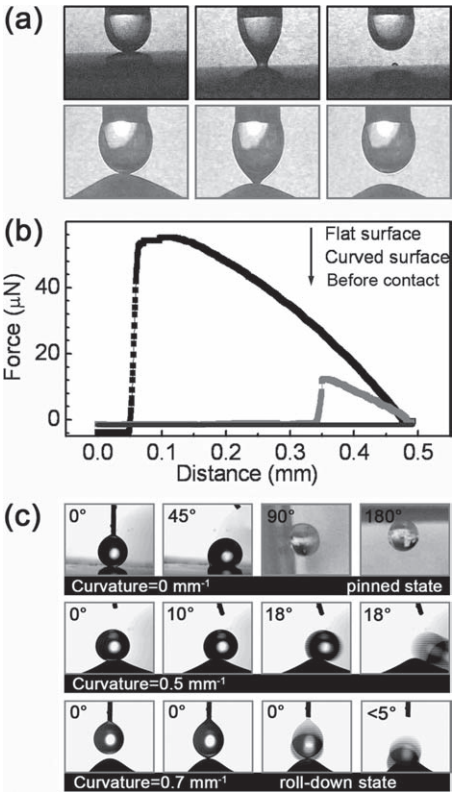

Figure 2. a) Adhesion force measurement between a water droplet and the samples. b) The force–distance curves recorded before and after the flat and curved superhydrophobic surfaces contacted with a droplet. c) Comparison of SA between flat and curved PDMS pillar arrays. A water droplet on a flat pillar array did not roll down even when the surface was tilted at 90° or 180°. A water droplet slides on a curved surface (curvature ca. 0.5 mm^{-1}) when the SA is about 18°. The water droplet could not stay on the larger curvature surface (curvature ca. 0.7 mm^{-1}) even when it was almost horizontal.

force between the water droplet and the flat surface is about 56 mN, while that for the curved surface is only 12.5 mN. Due to its strong adhesive force on the flat surface, a water droplet was snapped off from the 2 mm thick syringe (Figure 2a). In contrast, the water droplet could be easily dragged back without loss from the curved surface. Besides the adhesive property, sliding behavior, one of the most important parameters determining the superhydrophobic state, was also studied in this work. It could be clearly identified that the water droplet did not roll down when the tilt angle was 90° or even 180° (Figure 2c). However, with a small curvature (ca. 0.50 mm^{-1}) formed by a mechanical force, the water droplet rolled down with a SA of 18° (Figure 2c). When the curvature was further increased (>0.60 mm^{-1}), the water droplet could not stay on the surface even when it was almost horizontal (sliding angle <5°), indicating its good "roll-down" property.

According to the above experimental results, it is reasonable to reach the conclusion that the flat PDMS pillar array with high adhesion force is in the Wenzel superhydrophobic state. However, further investigation by in situ optical microscopy showed that there existed air in the interface between the pillars and the water droplet. When a water microdroplet was put onto a PDMS pillar array, the water expanded and gradually wetted the pillars under its weight and external pressure (Figure S4). This demonstrated that the pillar array was in a composite state despite its high adhesive force. Here, we call this new state the composite pinned state. In this case, the water droplet deeply infiltrated the upper region of the microstructure but still did not reach the bottom (**Figure 3a**, left). Generally, the larger the wetted region of the pillars, the stronger the adhesive force between the water droplet and the PDMS pillars, which is mainly caused by van der Waals forces. According to Wenzel's formula[35]

$$\cos\theta_W = r\cos\theta_Y \quad (1)$$

where θW is the apparent CA on a rough surface and θY is the ideal CA (Young's angle) of the water droplet on a smooth surface (θY = 110°, Figure S5). The roughness factor ($k = 1 + R\pi h_{eff}/d^2$) is defined as the ratio of the actual surface area to the projected area, where h_{eff} is the effectively wetted height of the pillars. According to the measured CA, about 150°, the wetted height of the pillars h_{eff} was calculated to be 1.9 μm. In other words, there is a 0.6 μm thick air layer at the bottom of the pillar array, which is consistent with the results derived from optical microscopy (Figure S4).

When a small curvature was formed on the external surface, the adhesion force between the surface and water droplet decreased significantly. The water droplet could roll down and the SA decreased by a certain degree, indicating the transitional superhydrophobic state (Figure 3a, center). When the curvature was further increased, the surface adhesion force decreased and the water droplet could roll down with SA less than 5°, indicating the Cassie superhydrophobic state (Figure 3a, right).[36] A possible reason for the unique change between pinned state and roll-down superhydrophobic state could be curvature-induced air injection into the pillar arrays Owing to the excellent flexibility of PDMS, the pillar array film could be alternated between a flat and a curved surface by an external force. Experimental results show that the wetting behavior of the surface also alternates between the roll-down state and pinned state. Moreover, different superhydrophobic states could be reversibly switched a large number of times by changing the surface curvature (Figure 3b).

Taking advantage of this unique switching between pinned and roll-down superhydrophobic states, we proposed an in situ "mechanical hand" for no-loss water droplet transportation. As shown in **Figure 4a**, a water droplet could be captured by flat PDMS pillar arrays easily owing to the strong adhesion force of the pinned superhydrophobic state. When a certain curvature was formed, a transition to the Cassie superhydrophobic state occurred, and the water droplet was released without mass

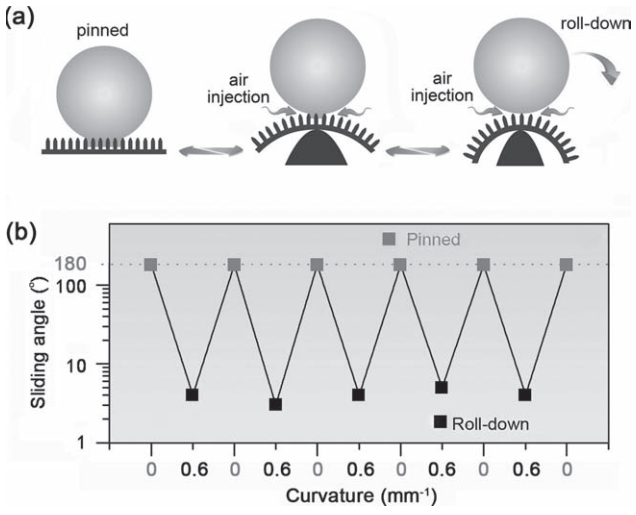

Figure 3. a) Scheme for reversible switching of three superhydrophobic states by curvature change. b) Reversible tests for the switching between pinned state and roll-down state.

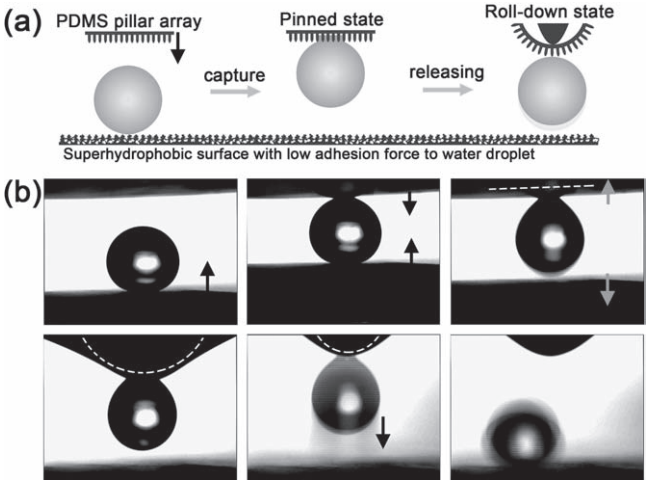

Figure 4. a) Scheme for water-droplet transport using curvature-driven switching between the pinned state and roll-down state. b) Process for capturing and releasing a water droplet. A water droplet can be captured by the flat PDMS pillar array without mass loss owing to its strong adhesive force. When the surface curvature was increased, the surface superhydrophobicity was tuned to the Cassie state, and the water droplet was released accordingly.

loss. Figure 4b shows the detailed working process of the water droplet transfer (Video S1 in the Supporting Information). A nanoporous poly(divinylbenzene) tablet was used as a superhydrophobic surface with low adhesion force for water droplet supply.[37] We believe that our in situ water transporter exhibits great potential for microfluidic and biomedical devices.

In conclusion, a simple curvature-driven in situ switching between pinned and roll-down superhydrophobic states has been proposed for the first time. To demonstrate the unique curvature tuning, a PDMS surface with a regular array of pillars was prepared by interference lithography and subsequent PDMS imprint lithography. Experimental results reveal that the CA increased to as large as 160° when the curvature increased. Moreover, the adhesion force and the SA show strong dependence on the surface curvature, giving the possibility of reversible switching between pinned and roll-down superhydrophobic states. Based on this unique switching, an in situ "mechanical hand" for no-loss water droplet transportation was proposed. This work provides a new insight into smart superhydrophobic surfaces with tunable wettability and exhibits refined control of water droplet mobility for biological and microfluidic applications.

Experimental Section

Materials and Equipment: PDMS Sylgard 184 was purchased from Dow Corning (MI). The epoxy negative resin SU-8 2075 was provided by NANO MicroChem Company (Newton, MA). A frequency-tripled, Q-switched, single-mode Nd:YAG laser with about 10 ns pulse width and 355 nm wavelength was purchased from Spectra-Physics (1791 Deere Avenue, Irvine CA 92606).

Preparation of PDMS Pillar Arrays: A two-beam laser interference microfabrication system was set up as reported earlier.[28] The SU-8 resin diluted with cyclopentanone (1:2 by volume) was spin-coated at 1000 rpm for 2.5 μm thickness. The sample was prebaked for 10 min to evaporate the organic solvent. Then the sample was exposed by two beams which were split from the UV laser (beam size ca. 9 mm, and laser power ca. 30 mW) to produce grating structures. After the sample had been rotated by 90°, it was exposed for the second time. The exposure time was 1 s in both cases. Then the sample was baked for 10 min and developed in the SU-8 developer for 5 min. After drying of the sample. a regular hole array template formed. The template was cast with PDMS prepolymer. Subsequently, the PDMS molds were cured in a conventional drying oven at 60 °C for 6 h. After the PDMS layer was peeled off, PDMS pillar arrays were obtained (Figures S1, S2).

Characterization: A 200 μm-diameter tip was pushed against the flexible PDMS film to produce a curved surface of the film. Different curvatures were obtained by different forces. The CAs were measured by Contact Angle Meter SL200B (Solon Tech., Shanghai). The morphologies of the PDMS pillar arrays were characterized by a field emission scanning electron microscope (JSM-7500F, JEOL, Japan). The adhesive force was measured by a high-sensitivity microelectromechanical balance system (Dataphysics DCA11, Germany). A 3 mL water microdroplet suspended on a hydrophobic metal ring were made to approach and retreat from the sample at 0.01 mm s^{-1} speed. Once the water droplet contacted the sample, it was dragged back. The balance force gradually increased, and reached a maximum before the droplet broke away from the sample.

Supporting Information

Supporting Information is available from the Wiley Online Library or from the author.

Acknowledgements

The authors gratefully acknowledge support from the NSFC under grant nos. 60525412, 90923037, and 60677016.

Received: May 8, 2010
Revised: August 17, 2010
Published online: November 12, 2010

[1] W. L. Min, B. Jiang, P. Jiang, *Adv. Mater.* **2008**, *20*, 3914.
[2] M. Nosonovsky, B. Bhushan, *Adv. Funct. Mater.* **2008**, *18*, 843.
[3] a) C. Greiner, E. Arzt, A. del Campo, *Adv. Mater.* **2009**, *21*, 479; b) J. Hong, W. K. Bae, H. Lee, S. Oh, K. Char, F. Caruso, J. Cho, *Adv. Mater.* **2007**, *19*, 4364.
[4] L. C. Gao, T. J. McCarthy, *Langmuir* **2006**, *22*, 2966.
[5] L. Zhai, F. C. Cebeci, R. E. Cohen, M. F. Rubner, *Nano Lett.* **2004**, *4*, 1349.
[6] I. A. Larmour, G. C. Saunders, S. E. J. Bell, *Angew. Chem. Int. Ed.* **2008**, *47*, 5043.
[7] L. J. Ci, S. M. Manikoth, X. S. Li, R. Vajtai, P. M. Ajayan, *Adv. Mater.* **2007**, *19*, 3300.
[8] Z. Z. Luo, Z. Z. Zhang, L. T. Hu, W. M. Liu, Z. G. Guo, H. J. Zhang, W. J. Wang, *Adv. Mater.* **2008**, *20*, 970.
[9] Z. Z Gu, H. Uetsuka, K. Takahashi, R. Nakajima, H. Onishi, A. Fujishima, O. Sato, *Angew. Chem. Int. Ed.* **2003**, *42*, 894.
[10] V. Jokinen, L. Sainiemi, S. Franssila, *Adv. Mater.* **2008**, *20*, 3453.
[11] P. Gould, *Mater. Today* **2003**, *6*, 44.
[12] B. Zhao, J. S. Moore, D. J. Beebe, *Science* **2001**, *291*, 1023.
[13] F. Z. Zhang, L. L. Zhao, H. Y. Chen, S. L. Xu, D. G. Evans, X. Duan, *Angew. Chem. Int. Ed.* **2008**, *47*, 2466.
[14] K. Ichimura, S. K. Oh, M. Nakagawa, *Science* **2000**, *288*, 1626.
[15] J. Lahann, S. Mitragotri, T. Tran, H. Kaido, J. Sundaram, I. S. Choi, S. Hoffer, G. A. Somorjai, R. Langer, *Science* **2003**, *299*, 371.
[16] L. Jiang, X. Feng, J. Liu, P. C. Rieke, G. E. Fryxell, *Macromolecules* **1998**, *31*, 7845.
[17] S. H. Anastasiadis, H. Retsos, S. Pispas, N. Hadjichristidis, S. Neophytides, *Macromolecules* **2003**, *36*, 1994.
[18] X. J. Feng, L. Feng, M. H. Jin, J. Zhai, L. Jiang, D. B. Zhu, *J. Am. Chem. Soc.* **2004**, *126*, 62.
[19] L. B. Xu, W. Chen, A. Mulchandani, Y. S. Yan, *Angew. Chem. Int. Ed.* **2005**, *44*, 6009.
[20] a) F. Xia, H. Ge, Y. Hou, T. L. Sun, L. Chen, G. Z. Zhang, L. Jiang, *Adv. Mater.* **2007**, *19*, 2520; b) X. Yu, Z. Q. Wang, Y. G. Jiang, F. Shi, X. Zhang, *Adv. Mater.* **2005**, *17*, 1289.
[21] a) N. Verplanck, E. Galopin, J. C. Camart, V. Thomy, Y. Coffinier, R. Boukherroub, *Nano Lett.* **2007**, *7*, 813; b) B. Kakade, R. Mehta, A. Durge, S. Kulkarni, V. Pillai, *Nano Lett.* **2008**, *8*, 2693.
[22] H. S. Lim, S. G. Lee, D. H. Lee, D. Y. Lee, S. Lee, K. Cho, *Adv. Mater.* **2008**, *20*, 4438.
[23] a) Y. Lai, X. Gao, H. Zhuang, J. Huang, C. Lin, L. Jiang, *Adv. Mater.* **2009**, *21*, 3799; b) C. Li, R. Guo, X. Jiang, S. Hu, L. Li, X. Cao, H. Yang, Y. Song, Y. Ma, L. Jiang, *Adv. Mater.* **2009**, *21*, 4254.
[24] G. Caputo, B. Cortese, C. Nobile, M. Salerno, R. Cingolani, G. Gigli, P. D. Cozzoli, A. Athanassiou, *Adv. Funct. Mater.* **2009**, *19*, 1149.
[25] W. H. Jiang, G. J. Wang, Y. N. He, X. G. Wang, Y. L. An, Y. L. Song, L. Jiang, *Chem. Commun.* **2005**, *28*, 3550.
[26] a) A. Lafuma, D. Quéré, *Nat. Mater.* **2003**, *2*, 457; b) S. T. Wang, L. Jiang, *Adv. Mater.* **2007**, *19*, 3423.
[27] X. Hong, X. F. Gao, L. Jiang, *J. Am. Chem. Soc.* **2007**, *129*, 1478.
[28] a) D. Wu, Q. D. Chen, H. Xia, J. Jiao, B. B. Xu, X. F. Lin, Y. Xu, H. B. Sun, *Soft Matter* **2010**, *6*, 263; b) S. Z. Wu, D. Wu, J. Yao, Q. D. Chen, J. N. Wang, L. G. Niu, H. H. Fang, H. B. Sun, *Langmuir* **2010**, *26*, 12012.

[29] W. K. Cho, I. S. Choi, *Adv. Funct. Mater.* **2008**, *18*, 1089.
[30] P. A. Quinto-Su, H. H. Lai, H. H. Yoon, C. E. Sims, N. L. Allbritton, V. Venugopalan, *Lab Chip* **2008**, *8*, 408.
[31] S. A. Lee, S. E. Chung, W. Park, S. H. Lee, S. Kwon, *Lab Chip* **2009**, *9*, 1670.
[32] D. Wu, Q. D. Chen, B. B. Xu, J. Jiao, Y. Xu, H. Xia, H. B. Sun, *Appl. Phys. Lett.* **2009**, *95*, 091902.
[33] a) H. B. Sun, A. Nakamura, S. Shoji, X. M. Duan, S. Kawata, *Adv. Mater.* **2003**, *15*, 2011; b) D. Wu, Q. D. Chen, J. Yao, Y. C. Guan, J. N. Wang, L. G. Niu, H. H. Fang, H. B. Sun, *Appl. Phys. Lett.* **2010**, *96*, 053704.
[34] M. H. Sun, C. X. Luo, L. P. Xu, H. Ji, Q. Ouyang, D. P. Yu, Y. Chen, *Langmuir* **2005**, *21*, 8978.
[35] R. N. Wenzel, *Ind. Eng. Chem.* **1936**, *28*, 988.
[36] A. B. D. Cassie, S. Baxter, *Trans. Faraday Soc.* **1944**, *40*, 546.
[37] Y. L. Zhang, S. Wei, F. J. Liu, Y. C. Du, S. Liu, Y. Y. Ji, T. Yokoi, T. Tatsumi, F. S. Xiao, *Nano Today* **2009**, *4*, 135.